

Elimination of cobalt (II) by adsorption on mesoporous materials and carbons of types SBA-15, CMI-1.

S. Boumessaïdia^{1,2,3}, B. Cheknane^{*2}, N. Bouchenafa-Saïb², K. Bachari³, F. Mekhales-Benhafsa³, O. Mohammedi².

¹Faculty of Exact Science, Hamma Lakhder University El Oued, Algeria.

²Laboratory Physical Chemistry of Interfaces of Materials Applied to the Environment, SaadDahleb University Blida, Algeria.

³Center for Scientific and Technical Research in Physico-Chemical Analysis, Bousmail Tipaza, Algeria.

*Corresponding author: ocheknane@yahoo.fr; Tel.: +213661849729; Fax: +21300 00 00

ARTICLE INFO

Article History :

Received : 26/01/2019

Accepted : 08/06/2019

Key Words:

Mesoporous materials;
cobalt (II);
Carbons;
Isotherms;
Kinetics adsorption.

ABSTRACT/RESUME

Abstract: This work aims to study the adsorption of a trace element (in our case we selected Cobalt (II)), on silicas and mesoporous coals of CMK-3 and CMK-3C type. These were made based on the synthesis of SBA-15 and CMI-1 as molds. Characterization of these materials was performed by X-ray diffraction, SEM and nitrogen adsorption-desorption (BET). The adsorptional properties of these materials were evaluated by studying the kinetics and adsorption isotherms of cobalt (II) metal ions. The Cobalt (II) adsorption experiments on the four matrices showed globally that the adsorption efficiencies of cobalt can be classified according to the order: CMK-3 > CMK-3C > CMI-1 > SBA-15, with efficiencies of 94.54%, 88.41% 76.09%, 74.07% respectively. Results of the cobalt adsorption kinetics modeling by the four materials in aqueous medium under optimal operating conditions is pseudo first order with adjustment coefficients ($R^2 > 0.98$). The adsorption isotherms clearly show that the Freundlich model is the most suitable for the different adsorption isotherms with adjustment coefficients ($R^2 > 0.97$).

I. Introduction

Nowadays, the problem of heavy metals has become more and more worrying. A common feature of industrial effluents is that they almost always contain toxic metals. The protection of the environment requires limiting the contents of these metals to the maximum allowed [1, 2]. Cobalt is an element found in all kinds of chemical compounds found in the environment. It is an earthy substance naturally present in minute amounts in soil, plants and food. In its pure state, cobalt is a hard, shiny metal with a steel gray or black color. It also exists as cobalt II and cobalt III, which form a number of organic and inorganic salts. Since cobalt is very present in the environment, humans can be exposed to it by breathing in the air, drinking water, or eating foods that contain cobalt. Skin contact with

soil or water containing cobalt may also increase exposure. Although not widely available in the environment, cobalt can be consumed by animals and plants if it's not associated with soils or sediments, resulting in the accumulation of this metal in the plants and animals. Thus, there can be a significant accumulation of cobalt in plants and animals. Several treatment processes have been tried to eliminate these pollutants such as adsorption [3].

Several adsorbents are used for the treatment of these waters such as silicic mesoporous materials, which are also used for the synthesis of other adsorbents such as mesoporous coals[4].

After the discovery of MCM materials by Mobil researchers in 1992 [5], much research has been done to synthesize all sorts of mesoporous siliceous materials.

The efforts made on the synthesis of these mesoporous siliceous materials have resulted in a wide range of materials with different pore structures, pore diameters, stabilities and adsorption capacities. For example SBA-15, synthesized by Zhao et al. [6,7], is one of the most studied mesoporous silica supports because of its easy synthesis and its good thermal and hydrothermal stability. SBA-15 has large uniform adaptable pores (3-15 nm), thick walls of amorphous silica (3-6 nm) and high surfaces (700-800 m²/g).

The use of coal in the adsorption process is also very much in demand. Activated carbon has a high adsorption capacity due mainly to its large surface area. In 1999, Ryoo et al. succeeded in synthesizing the first ordered mesoporous carbon based on the nanocasting process [8]. Generally, the synthesis of mesoporous carbons from the mesoporous silica can be described as follows: an acidic solution of the carbon precursor is impregnated into the pores of the silica. Then, polymerization followed by carbonization of this precursor at high temperature results in the creation of the "carbon-silica" composite and the final carbonaceous matrix is obtained after complete dissolution of the silica by HF or NaOH. The most commonly used carbon precursors are sucrose [4], furfuryl alcohol [9], phenolic resins [10], divinylbenzene [11], acrylonitrile [12], pyrrole [13] ... These mesostructured carbons have many applications: supports in catalysis [14], adsorbents [15], storage of hydrogen [16], manufacture of electrodes [17]. The present work concerns the comparative study of the adsorption capacity of the Co²⁺ metal ion on the CMI-I, SBA-15 type mesostructured materials and the mesoporous coals synthesized from CMI-1 and SBA-15.

II. Experimental

II.1. Synthesis of Mesostructured Silicas

II.1.1. CMI-1

The synthesis protocol of the conventional CMI-1 material involves the preparation of a 10% by weight solution of decaoxyethylenecetyl ether surfactant in 60 ml of bi-distilled water at 70 °C for 3 hours with stirring. Adjusted at pH = 2 by the addition of H₂SO₄ [18].

Tetramethoxysilane (T'MOS), the source of silica is added dropwise to the solution. The surfactant / silica molar ratio is set at 0.50. After 1 h, the gel obtained is cast in a Teflon sheath which is sealed in an autoclave to undergo a heat treatment for 3 days at 80 °C under static conditions.

The gel obtained after treatment is then filtered, washed with distilled water and dried. The synthesis ends with the calcination of the material obtained at 550 °C. with a rise of 2 °C/min, followed by a plateau of 6 hours at the final temperature.

II.1.2. SBA-15

The synthesis of the SBA-15 materials used for this work was carried out according to the protocol described by Zhao and his collaborators [19]:

The synthesis is described as follows: 5.0 g of Pluronic P123 are dissolved in a mixture of 115 ml of bidistilled water and 3.5 ml of HCl 32%. This mixture is brought to 40 °C and stirred. When all the surfactant is dissolved, 13 g of tetraethoxysilane (TEOS) is added dropwise. Once the silica source has been added, the solution is maintained at 40 °C with constant stirring for 24 hours.

The gel obtained is subjected to a heat treatment of 100 °C for 24 hours. then filtered, washed with distilled water and finally dried. The synthesis ends with the calcination of the material obtained at 550 °C with a rise of 1 °C/min followed by a plateau for 6 hours of the final temperature.

II.2. Synthesis of mesostructured carbons

The synthesis of mesoporous coals used for this work was carried out according to the mechanism of nanocasting. The principle of this mechanism is summarized by three synthesis steps, the first is the formation of the rigid mold (in our case the SBA-15 and the CMI -1), the second step is the formation of a composite by impregnating the pores of the rigid mold with a precursor of the desired material and finally removing the rigid mold to obtain the desired replica [4].

CMK-3 and CMK-3C are obtained following the replication of the pure mesoporous silica (SBA-15 and CMI-1 respectively). 1.25 g of sucrose are dissolved in 5 ml of H₂SO₄ (0.28 M). The resulting solution is introduced into 1 g of pure silica and the whole is heated in air at 100 °C for 6 h and then at 160 °C for 6 h. A second impregnation is then carried out by introducing 5 ml of the sucrose solution in H₂SO₄ (0.18 M containing 0.8 g of sucrose). Likewise, the mixture obtained is heated at 100 °C for 6 hours and then at 160 °C for 6 hours. The recovered black solid is pyrolyzed at 900 °C for 8 hours. The composite "SiO₂ / C" is immersed for 24 hours in 80 ml of a 5% solution of HF to remove the silica. The resulting carbon is then filtered, washed with water and air-dried at room temperature for 24 hours [20].

III. Characterization

The characterization of our materials was carried out by X-ray diffraction, nitrogen adsorption-desorption (BET) and scanning electron microscopy (SEM).

III.1. X-ray diffraction

The small-angle diffractogram (FIG. 1) of 0.75 to 3.5° of the CMI-1 silica exhibits a first peak of intense diffraction observed at 1.73° and of two other small peaks not visible at 3.2° and 3.6°, and for the SBA-15 the presence of a main peak at

1.54° and two smaller placed around 2° to 1.65° and 2.42° respectively. The first peak represents the reflection of the plane (100) and the other two of the planes (110) and (200). This demonstrates the formation of organized porous networks [21].

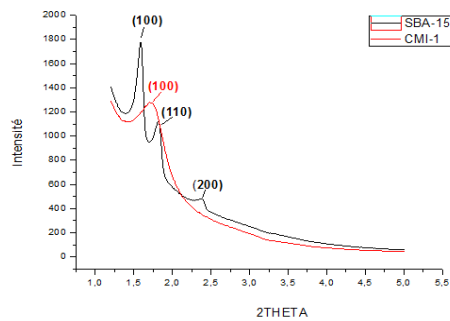


Fig 1. X-ray diffractograms of CM-1 and SBA-15 at low angles.

They can be indexed to count the reflections hkl (100), (110) and (200) associated with the hexagonal symmetry P6mm [22]. The regularity of the channels is two-dimensional, in a plane perpendicular to the axis of the cylindrical channels, which explains that the third index of Miller is always zero.

From this analysis, we have been able to determine the interdeictular distances dhk1 and the mesh parameters a_0 for the two silicas ($a_0 = 2 / \sqrt{3} \cdot d_{100}$). We used the inter-plane distance between the planes (100) to calculate the corresponding mesh parameters. Table 1 summarizes the results obtained.

FIG. 2 represents the diffractograms of the two carbonaceous replicas obtained from the silicic molds. The peaks observed are characteristic of

solids in which the pores are regular and ordered. These two carbon appear between 1.5° and 3.5° (2θ) and are attributed to Miller's (100), (110), (200) lattice planes; this confirms that CMK-3 and CMK-3C admits the same hexagonal arrangement of mesopores as its SBA-15 and CMI-1 mold (P6mm symmetry) [21].

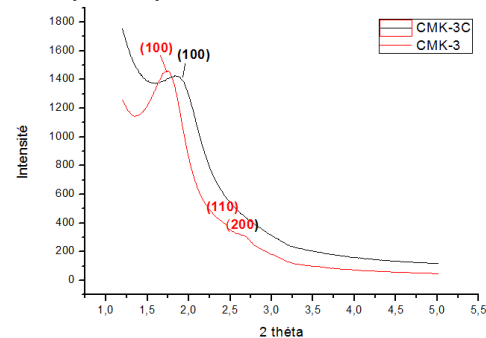


Fig 2. X-ray diffractograms of CMK-3 and CMK-3C at low angles.

The mesh parameters of the carbonaceous networks CMK-3 and CMK-3C are calculated respectively from the interticular distances (100) (Table 1). These values are smaller than those obtained on their respective molds 5.04 and 4.20 nm respectively for SBA-15 and CMI-1. This decrease, of the order of (0.7-0.9 nm), is due to the contraction of the structure under the effect of the heat treatment applied at high temperature (900 °C) to develop the carbon.

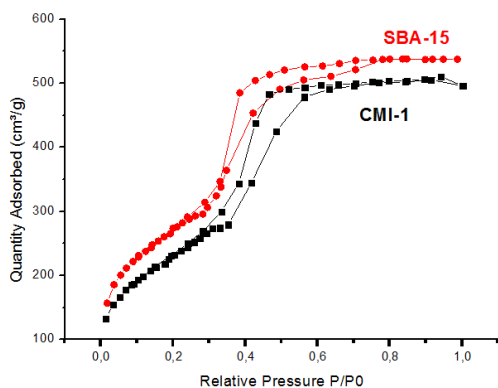
Table 1. Structural properties of silicas and synthesized coals

Silica and carbons	d (nm)	a_0 (nm)
SBA-15	5.76	6.65
CMI-1	5.07	5.85
CMK-3	5.04	5.81
CMK-3C	4.20	4.85

III.2. Nitrogen adsorption-desorption porosimetry at 77 K (BET analysis)

The textural properties of our materials were determined from the isotherm of nitrogen adsorption / desorption at low temperature (77K). Figure 3 shows the characteristic isotherms of the

silicas studied. They are all of type (IV) according to the classification (IUPAC), which confirms the mesoporosity of our materials [23-24]. The hysteresis loops, which appear more clearly in the SBA-15 and CMI-1 isotherms, correspond to an H1



type hysteresis. The mesopores of our silicic materials are therefore uniform in size.

Fig 3. Curves of nitrogen adsorption / desorption isotherms of silicas studied.

On the other hand, our silicas have a high specific surface (601-833 m²/g) (Table 3) so they are very good supports for the adsorption of heavy metals. As for the molds, the nitrogen adsorption / desorption isotherm curves of the carbons represent mesoporous solids because they are type IV according to the IUPAC classification (Figure 4). The branches of adsorption and desorption of nitrogen indicate that the quantities of gas (N₂) adsorbed and desorbed on the surface of our carbons are not equivalent and thus hysteresis loops

appear. These, which reflect the difference between capillary condensation (adsorption) and evaporation (desorption), are of type H1.

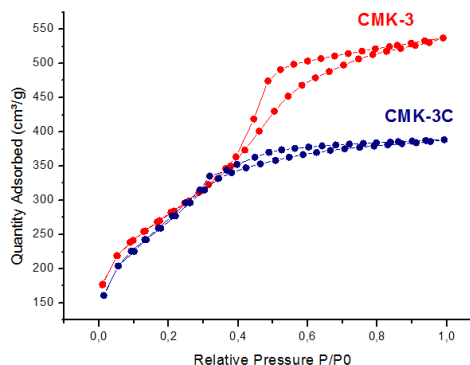


Fig 4. Curves of adsorption / desorption nitrogen isotherms studied carbons.

The textural properties (SBET, dpetVmeso) of mesoporous carbons CMK_n are summarized in Table 3. The carbons are characterized by high specific surfaces calculated by BET (999.01 - 1071 m²/g). These surfaces surpass those of the respective silicas (SBET = 833 and 624m²/g for CMI-1 and SBA-15 respectively), because the carbon density is lower than that of silica and additional pores can be created during pyrolysis.

Table 2. The different values of specific surface area and pore size obtained.

Enchantions	Specific surface (m ² /g)	Pore diameter (nm)	Pore volume (cm ³ /g)
SBA-15	601	4.4	0.92
CMI-1	833	3.2	0.76
CMK-3	1071.84	2.3	0.83
CMK-3C	999.01	2.4	0.70

III.3. Thickness of the walls

Wall thickness is estimated by combining the results of diffraction and nitrogen adsorption / desorption techniques, referred to as "e". In the case of hexagonal symmetry (P6mm), this is the difference between the mesh parameter and the pore diameter (e = a₀ - dp). Table 3 shows the wall thickness values for the four materials considered.

The two coals CMK-3 and CMK-3C were obtained by mesoporous silica replication, the thickness of the walls of the starting silica must correspond to the pore size of the coal, this hypothesis is perfectly verified. Indeed, they have a pore diameter of value (dp = 2.3 nm and 2.4 nm for CMK-3 and CMK-3C) are comparable to that of the thickness of the wall of their silicic mold (e = 2, 25 nm and 2.65 nm for SBA-15 and CMI-1) with a difference not exceeding 0.25 nm.

Table 3. Structural parameters of mesoporous materials obtained by association DRX-Adsorption / desorption of nitrogen.

Enchantions	a_0 – DRX (nm)	Pore diameter (nm)	e (nm)
SBA-15	6.65	4.4	<u>2.25</u>
CMI-1	5.85	3.2	2.65
CMK-3	5.81	<u>2.3</u>	3.51
CMK-3C	4.85	2.4	2.43

III.4. Scanning Electron Microscopy Analyzes (SEM)

The Scanning Electron Microscopy Analyzes is an electron microscopy technique capable of producing high resolution images of the surface of a sample using the principle of electron-matter interactions. This technique is to confirm that the synthesized coals are the same morphology of their silicic mold, Figure 5 shows the SEM images of the four adsorbents, these images shows that each of the two charcoal keeps the same morphology of its silicate mold, cylindrical morphology for SBA -15 [25] and CMK-3 and spherical morphology for CMI-1 [26] and CMK-3C.

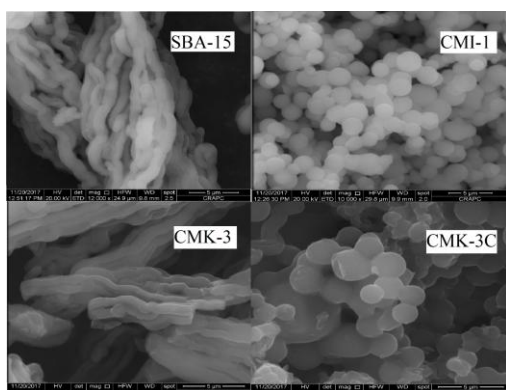


Fig 5. Images Adsorption analyzes by scanning electron microscopy.

IV. Application in adsorption

The adsorption of cobalt on materials SBA-15, CMI-1 and their synthesized carbons was studied in static mode. Experiments were performed at room temperature and a neutral pH under different operating conditions. The effects of adsorbent mass and contact time were evaluated. At the end of the equilibrium period, the amounts of residual metal

are determined by atomic absorption spectrometry (AAS).

IV.1. Effect of contact time

The effect of contact time on cobalt removal was evaluated to demonstrate the time required to reach the adsorption equilibrium. The experiments were carried out under the same operating conditions described above: 10 mg of adsorbent was added to 5 ml of cobalt solution (11.4 mg / L, pH 6.4) and the mixture was stirred at 250 ° C. RPM Samples for analysis were taken at regular time intervals to determine the residual cobalt concentration. The results obtained are shown in Figure 6 show that the cobalt adsorption process generally has two phases: a rapid initial phase where the adsorption capacity increases sharply in the first 60 minutes due to the existence of a free surface and a slow second phase associated with the internal surface adsorption. The results obtained show that the adsorption equilibrium can be reached after a contact time of about 100 minutes. After that, the adsorption percentage did not change with a further increase in contact time because the amount of adsorbed cobalt reached a stable state with the amount of residual metal in the solution.

The adsorption kinetics for each adsorbent is illustrated in Figure 6. Obtained by plotting the adsorbed quantity Q_e versus time, $Q_e = f(t)$.

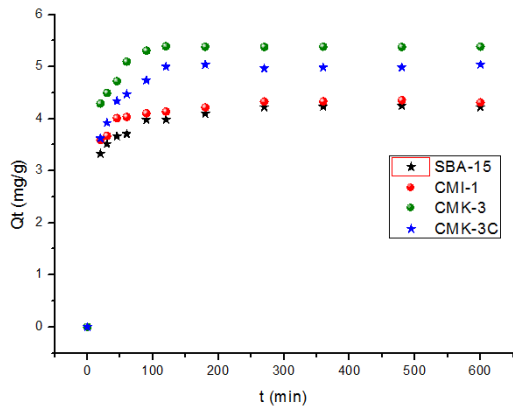


Fig.6. Cobalt adsorption kinetics on adsorb.

The maximum adsorption rates of cobalt (II) are of the order of 76.09% (4.33 mg / L) for CMI-1, 74.07% (4.22 mg / L) for SBA -15, 88.41% (5.03 mg / L) for CMK-3C and 94.54% (5.38 mg / L) for CMK-3.

IV.1.1. Modeling of cobalt adsorption kinetics

The adsorption of heavy metals from the liquid phase to the solid phase can be considered as a reversible equilibrium reaction between the two

phases [27]. Lagergren's pseudo-first order model [28], equation (1), and pseudo-second order model of Ho [29], equation (2), were applied to the data.

$$q = q_e(1 - e^{-k_1t}) \tag{1}$$

$$q = \frac{q_e^2 k_2 t}{1 + q_e k_2 t} \tag{2}$$

When Q_e and q (mg g^{-1}) are the amount of cobalt adsorbed at equilibrium and the time t (min), k_1 (min^{-1}) is the pseudo-first rate constant and k_2 ($\text{g mg}^{-1}\text{min}^{-1}$) is the pseudo-second order model speed constant.

As can be seen, the first-order equation provided a better-tuned model than the second-order equation with a high correlation coefficient that is very close to unity ($R^2 > 0.98$). It was found that the pseudo-first order model gave perfect fits to the experimental data. The calculated Q_e values agree well with the experimental data, we conclude that the kinetics of adsorption of cobalt by the four materials is pseudo first order. Also adds that the speed constant is greater with the CMI-1 in both models.

Table 4: Kinetic parameters of both models.

adsorbants	Q_e (exp)	pseudo-first order model			pseudo-second order model		
		Q_e	K_1	R^2	Q_e	K_2	R^2
SBA-15	4.09	4.07	0.072	0.988	4.25	0.036	0.977
CMI-1	4.33	4.21	0.083	0.994	4.35	0.048	0.979
CMK-3	5.38	5.31	0.069	0.994	5.51	0.030	0.972
CMK-3C	4.99	4.93	0.031	0.978	5.30	0.009	0.958

IV.2. Effect of initial adsorbent concentration

The effect of the initial concentration provides an important driving force for overcoming the mass transfer resistance of the metal between the aqueous and solid phases. The effect of the initial concentration is studied by adding mass of 5 to 50 mg of each adsorbent to 5 ml of cobalt (II) solutions at 11.4 mg/L concentration. The experiments were conducted at room temperature and normal pH of the cobalt solution (pH 6.4) and at a stirring speed of 250 rpm for 1 hour. Residual concentrations and adsorbate amounts per unit mass of adsorbent were determined. The evolution of Q (mg / g) as a function of the initial concentration of cobalt is shown in FIG. 7.

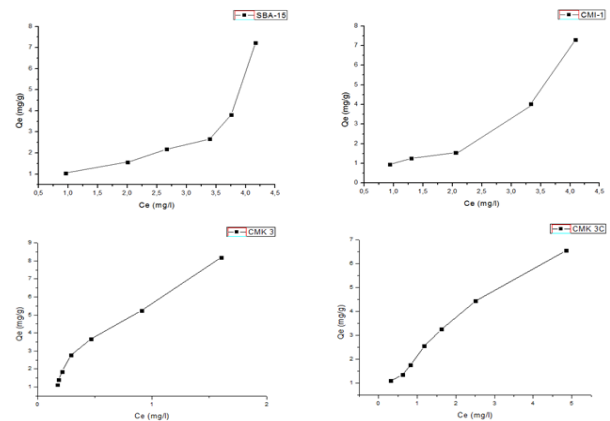


Fig 7. Cobalt adsorption isotherms.

According to the classification Giles et al [30]. The curves obtained show that the isotherm of the CMK-3 and CMK-3C coals is of type L. This curve can be mathematically described by the Langmuir or Freundlich equation. The more sites occupied by solute molecules, the more difficult the adsorption of new molecules.

The isotherm of materials SBA-15 and CMI-1 is of type S. The amount of cobalt Co^{+2} adsorbed is practically zero at a low concentration of solution, because the concentration of the solution increases the adsorbed quantity increases rapidly. Thus, the adsorbed molecules promote the subsequent adsorption of other molecules (cooperative adsorption due to the attraction between the molecules of the solute by Van der Waals forces).

IV.2.1. Modeling of adsorption isotherms

The adsorption isotherms in our case were analyzed using the models Langmuir [31], Equation (3) and Freundlich [31], Equation (4).

$$q_e = q_m \frac{k_L C_e}{1 + k_L C_e} \quad (3)$$

$$q_e = k_F C_e^n \quad (4)$$

Where Q_e is the adsorption capacity at equilibrium (mg / g), Q_m is the maximum adsorption capacity (mg / g), It is the residual concentration of adsorbate at equilibrium (mg / L), K_L is the Langmuir constant (L / mg), K_F is a constant indicative of the adsorption capacity of the adsorbent and n is an empirical constant related to the amplitude of the adsorption driving force. non-linear regression were performed using Origin 8.1. The essential characteristics of the Langmuir isotherm can be expressed in terms of the non-dimensional constant separation factor R_L given by the following equation:

$$R_L = \frac{1}{1 + K_L C_0} \quad (5)$$

There are four probabilities for the R_L value: favorable sorption ($0 < R_L < 1$); unfavorable sorption ($R_L > 1$); linear sorption ($R_L = 1$) and irreversible sorption ($R_L = 0$).

Modeling has shown that the Langmuir model adapts very well to the experimental points with the two coals, and that the value of the correlation parameter is close to 1 ($R^2 > 0.97$). The calculated value of R_L is less than 1, to conclude that the adsorption of Co^{2+} is favorably carried out on the two coals to be studied. On the other hand, in the case of the two materials SBA-15 and CMI-1, the calculated value of R_L is almost equal to 1 (> 0.993), which shows that the adsorption with this model is linear for siliceous materials.

On the other hand, the value of the correlation parameter R^2 is close to 1 ($R^2 > 0.92$), which makes it possible to deduce that the Freundlich model is applicable to the adsorption of cobalt by the four adsorbents.

For the SBA-15 and CMI-1 matrices, the value of $(1 / n)$ obtained by applying the Freundlich model to our experimental results is greater than 1 ($1 / n = 2.7$ and 1.86 successively). This shows that the isotherms are of type S.

These experimental results show that the Freundlich model is reliable. At low solute concentrations, the adsorption remains lower and becomes larger as the concentration of cobalt (II) increases, confirming that solute-solute interactions are stronger than solute-adsorbent interactions.

The value of the parameter $1 / n$ obtained by the Freundlich model is less than 1 in the case of the two coals, which shows that the isotherms are of type L. The results obtained experimentally in the Freundlich model perfectly describe the process of adsorption for cobalt on CMK-3 and CMK-3C.

The overall results of the different models of adsorption isotherms are summarized in Table 5

Table 5. Isotherm parameters of the Freundlich and Langmuir model

Parameters of models		SBA-15	CMI-1	CMK-3	CMK-3C
Langmuir	K_L (L/mg)	$4.47 \cdot 10^{-5}$	$4.29 \cdot 10^{-5}$	0.52	0.19
	Q_m (mg/g)	25118	31281	17.65	13.45
	R^2	0.80	0.89	0.97	0.99
	R_L	0.995	0.993	0.14	0.31
Freundlich	K_f (mg/g)	0.132	0.49	5.8	2.22
	$1/n$	2.7	1.86	0.73	0.69
	R^2	0.92	0.97	0.99	0.99

V. Conclusion

The application of CMI-1, SBA-15, CMK-3 and CMK-3C to the adsorption of cobalt (II) ions was examined in their retention capacities vis-à-vis this metal. The maximum adsorption rates of cobalt (II) are of the order of 76.09% (4.33 mg / L) for CMI-1, 74.07% (4.22 mg / L) for SBA-15, 88.41% (5.03%) mg / L for CMK-3C and 94.54% (5.38 mg / L) for the CMK-3.

The curves of the isotherms obtained show that the isotherm of the CMK-3 and CMK-3C are of the type, and the isotherm of the SBA-15 and CMI-1 materials are of the S type. The adsorption isotherms of Co^{2+} on the oven is modeled using Langmuir and Freundlich isotherms. Adsorption isotherms of Co^{2+} on the solids are modeled using the isotherms of Langmuir and Freundlich. Results of monetization using the nonlinear regression method shows, that these models can describe the adsorption phenomenon onto the furnace matrices ($R^2 > 0.9$); except in the case of the Langmuir model which is applicable only to CMK-3 and CMK-3C carbons. All the results show that the adsorption efficiency of cobalt is higher than that of the CMK-3, which has a higher surface area than the other matrices.

VI. References

- Volesky, B. Detoxification of metal-bearing effluents: biosorption for the next century. *Hydrometallurgy* 59(2001) 203–216.
- Demim, S.; Drouiche, N.; Aouabed, A.; Benayad, T.; Dendene Badache, O. Cadmium and nickel: Assessment of the physiological effects and heavy metal removal using a response surface approach by L. gibba. *Ecological Engineering Elsevier* 61 (2013) 426–435.
- Stoeckli, F.; Lavanchy, A.; Hugi-Cleary, D. *Fundamentals of Adsorption*. Paris : Elsevier (1998) 75–80.
- Lu, A-H.; Schüth, F. Nanocasting: A Versatile Strategy for Creating Nanostructured Porous Materials. *Advanced Materials* 18 (2006) 1793–1805.
- Kresge, J S.; Leonowicz, M E.; Roth, W J.; Beck, J C. Ordered mesoporous molecular sieves synthesized by a liquid-crystal template mechanism. *Nature* 359 (1992) 710–712.
- Zhao, D.; Feng, J.; Huo, Q.; Melosh, N.; Fredrickson, G H.; Chmelka, B F.; Stucky, G D. Triblock copolymer syntheses of mesoporous silica with periodic 50 to 300 Angstrom pores. *Science* 279 (1998) 548–552.
- Zhao, D.; Huo, Q.; Feng, J.; Chmelka, B F.; Stucky, G D. Nonionic triblock and star diblock copolymer and oligomeric surfactant syntheses of highly ordered, hydrothermally stable, mesoporous silica structures. *Journal American Chemistry Society* 120 (1998) 6024–6036.
- Ryoo, R.; Joo S H.; Jun, S. Synthesis of highly ordered carbon molecular sieves via template-mediated structural transformation. *Journal Physique Chemistry* 103(1999) 7743–7746.
- Joo, S H.; Choi, S J.; Oh, I.; Kwak, J.; Liu, Z.; Terasaki, O.; Ryoo, R. Ordered nanoporous arrays of carbon supporting high dispersions of platinum nanoparticles. *Nature* 412 (2001) 169–172.
- Lee, J.; Yoon, S.; Hyeon, T.; Oha, S M.; Kimb, K. B. Synthesis of a new mesoporous carbon and its application to electrochemical double-layer capacitors. *Chemistry Communications* (1999) 2177–2178.
- Yoon, S B.; Kim, J Y.; Yu, J S. A direct template synthesis of nanoporous carbons with high mechanical stability using as-synthesized MCM-48 hosts. *Chemistry Communications* (2002) 1536–1537.
- Lu, A.; Kiefer, A.; Schmidt, W.; Schüth, F. Synthesis of polyacrylonitrile-based ordered mesoporous carbon with tunable pore structures. *Chemistry Materials* 16 (2004) 100–103.
- Yang, C M.; Weidenthaler, C.; Spliethoff, B.; Mayanna, M.; Schüth, F. Facile template synthesis of ordered mesoporous carbon with polypyrrole as carbon precursor. *Chemistry Materials* 17 (2005) 355–358.
- Rodríguez-Reinoso, F. The role of carbon materials in heterogeneous catalysis. *Carbon* 36 (1998) 159–175.
- Peng, X.; Cao, D.; Zhao. Grand canonical Monte Carlo simulation of methane-carbon dioxide mixtures on ordered mesoporous carbon CMK-1. *Journal of Separation and Purification Technology* 68(2009) 50–60.
- Xia, K.; Gao, Q.; Song, S.; Wu, C.; Jiang, J.; Hu, J.; Gao, L. CO_2 activation of ordered porous carbon CMK-1 for hydrogen storage. *International Journal Hydrogen Energy* 33(2008) 116–123.
- Flandrois, S.; Simon, B. Carbon materials for lithium-ion rechargeable batteries. *Carbon* 37 (1999) 165–180.
- Blin, J L.; Ldonard, A.; Su, B L. Well-Ordered Spherical Mesoporous Materials CMI-1 Synthesized via an Assembly of Decaoxyethylene Cetyl Ether and TMOS. *Chemistry Materials* 13(2001) 3542–3553.
- Schmidt-Winkel, P.; Lukens, W.; Yang, J P.; Margolese, D I.; Lettow, J S.; Ying, J Y.; Stucky, G D. Microemulsion Templating of Siliceous Mesostructured Cellular Foams with Well-Defined Ultralarge Mesopores. *Chemistry Materials* 12 (2000) 686–696.
- Lignier, P.; Comotti, M.; Schüth, F.; Rousset J.-L.; Caps, V. Effect of the Titania morphology on the Au/TiO₂-catalyzed aerobic epoxidation of stilbene. *Catalysis Today* 141(2009) 355–360.
- Kerdi, F.; Caps, V.; Alain, T. Mesostructured Au/C materials obtained by replication of functionalized SBA-15 silica containing highly dispersed gold nanoparticles. *Microporous and Mesoporous Materials* 140 (2011) 89–96.
- Meynen, V.; Cool, P.; Vansant, E F. Verified Syntheses of Mesoporous Materials. *Microporous and Mesoporous Materials* 125(2009) 169–224.
- Impérator-Clerc, M.; Davidson, P.; Davidson, A. Existence of a Microporous Corona around the Mesopores of Silica-Based SBA-15 Materials Templated by Triblock Copolymers. *Journal American Chemistry Society* 122 (2000) 11925–11933.
- Jermy, B R.; Cho, D R.; Bineesh, K V.; Kim, S Y.; Park D W. Direct synthesis of vanadium incorporated three-dimensional KIT-6: A systematic study in the oxidation of cyclohexane. *Microporous and Mesoporous Materials* 115 (2008) 281–292.
- De Witte, K.; Busuioc, A.M.; Meynen, V.; Mertens, M.; Bilba, N.; Van Tendeloo, G.; Cool, P.; Vansant, E.F. Influence of the synthesis parameters of TiO₂-SBA-15 materials on the adsorption and photodegradation of rhodamine-6G. *Microporous and Mesoporous Materials* 110 (2008) 100–110.
- Stébé, M.J.; Emo, M.; Fornly-Le Follotec, A.; Metlas-Komunjer, L.; Pezron, I.; Blin, J. L. Triblock siloxane copolymer surfactant: Template for spherical mesoporous silica with a hexagonal pore ordering. *Langmuir* 29 (2013) 1618–1626.
- Onundi, Y. B.; Mamun, A.; Al Khatib, M. F.; Ahmed, Y. M. Adsorption of copper, nickel and lead ions from synthetic semiconductor industrial wastewater by palm shell activated carbon. *International journal Environment Science and Technology* 17 (2010) 751–758.

28. Lagergren, S. About the Theory of So-Called Adsorption of Soluble Substances. *Kungliga Svenska Vetenskapsakademiens Handlingar*, 24 (1898) 1-39.
29. Ho, Y.S.; McKay, G. Pseudo-second order model for sorption processes. *Process Biochemistry* 34 (1999) 451-465.
30. Senthil Kumar, P.; Kirthika, K. Equilibrium and kinetic study of adsorption of nickel from aqueous solution onto bael tree leaf powder. *Journal of Engineering Science and Technology* 4 (2009) 351-363.

Please cite this Article as:

Boumessaidia S., Cheknane B., Bouchenafa-saib N., Bachari K., Mekhales Benhafsa F., Mohammedi O., *Elimination of cobalt (II) by adsorption on mesoporous materials and carbons of types SBA-15, CMI-1, Algerian J. Env. Sc. Technology, 5:3 (2019) 1046-1054*